

## *Effect of Air Outlet Angle on Air Distribution Performance Index*

Dr. Isbeyeh W. Maid  
Assist. Prof.  
Tech. College Baghdad

Dr. Ahmed A. M. Saleh  
Lecturer  
Univ. of Technology

Nasser I. Khalaf  
Engineer  
North Ref. Company

### **Abstract:**

In this paper a numerical study of velocity and temperature distribution in air conditioned space have been made. The computational model consists of the non-isothermal 3-D turbulent with (k-ε) model. The numerical study is made to conduct air distribution in a room air-conditioned space with real interior dimensions (6×4×3)m and to analyze the effect of changing angle of grille vanes on the flow pattern, velocity, and temperature distribution in the room under a set of different condition, and under a supply air temperature of 16°C to examine the final result on air distribution performance index (ADPI).

The results show a significant effect within the change of supply air angle, the maximum air distribution performance index (ADPI) is 52% when air change per hour (ACH) is equal to 10 at 16°C inlet temperature with angle ( $\theta = 15^\circ$  down), and the minimum value of (ADPI) is 20% when ACH is equal to 15 at 16°C inlet temperature and angle ( $\theta = 0$  degree).

**Keywords:** Air Outlet Angle, Air Distribution Performance Index (ADPI), k-ε Model.

تأثير زاوية انحراف زعانف مدخل الهواء على قيمة معامل أداء توزيع الهواء

الخلاصة

تناول هذا البحث دراسة عددية لتوزيع درجات الحرارة والسرعة للهواء في الفضاءات المكيفة. تضمنت الدراسة العددية توزيع الهواء في الفضاءات المكيفة ذات التصاميم الإنشائية الحقيقية وتأثير زاوية انحراف زعانف مدخل الهواء على هيئة الجريان وتوزيع السرعة ودرجات الحرارة في الغرفة ودراسة موقع فتحة التجهيز وفتحة الهواء الراجع عند معدلات مختلفة من تغير الهواء في الساعة ( 5,10,15 ACH ) ودرجات حرارة تجهيز للهواء مقدارها 16 °C وتأثير ذلك على قيمة معامل أداء توزيع الهواء (ADPI). ولغرض انجاز هذه الدراسة تم تطوير برنامج حسابي بلغة الفورتران وحل معادلة (k-ε) لنمذجة الاضطراب والفرقات المحددة. أظهرت النتائج بأن أفضل توزيع لدرجات الحرارة والسرعة هي عندما تكون درجة حرارة الهواء المجهز (16°C) وعدد مرات تغير الهواء بالساعة (ACH = 10) وزاوية انحراف زعانف مدخل الهواء ( $\theta = 15^\circ$  down) حيث كانت قيمة معامل أداء توزيع الهواء (ADPI) تساوي 52%، بينما اقل قيمة لمعامل أداء توزيع الهواء حصلت عند (ACH = 5) ودرجة حرارة التجهيز (16 °C) وبزاوية (0 درجة).

## Notations

$A_{inlet}$ : Area of Inlet ( $m^2$ ).  
 $A_{outlet}$ : Area of Outlet ( $m^2$ ).  
 $C_p$  : Specific Heat Capacity at Constant Pressure ( $J/kg. K^o$ ).  
 $F_1, F_2, F_\mu, E$  : Empirical Function i k- $\epsilon$  Model  
 $g$  : Gravity ( $m/s^2$ ).  
 $H$  : Room Height ( m).  
 $I_u^2$  : Turbulent Intensity of the X-Velocity.  
 $k$  : Turbulent Kinetic Energy (Joul).  
 $k_{in}$  : Turbulent Kinetic Energy at Inlet (Joul).  
 $P$  : Pressure ( $N/m^2$ ).  
 $T$  : Temperature ( $^oC$ ).  
 $t$  : Time (sec).  
 $U, V, W$  : Velocity Components in X, Y & Z (m/s).  
 $u, v, w$  : Turbulent Components.  
 $U$  : Mean Velocity Component (m/s).  
 $U_{in}$  : Inlet Velocity ( m/s).  
 $U_{out}$  : Outlet Velocity (m/s).  
 $U_n$  : Normal Velocity (m/s).

ACH : Air Change per Hour.  
 $C_1, C_2, C_\mu$  : Constant Coefficient in k- $\epsilon$  Model.

$U_t$  : Tangential Velocity (m/s).

## Greek Symbols

$\alpha$  : Thermal Diffusivity ( $m^2/s$ ).  
 $\beta$  : Thermal Expansion coefficient (1/K).  
 $\Delta X_i, \Delta Y_j, \Delta Z_k$  : Distance between Scalar Quantities.  
 $\delta_{ij}$  : Kronecker Delta.  
 $\sigma_k$  : Empirical Constant = 1.0  
 $\epsilon$  : Turbulent Energy Dissipation Rate.  
 $\epsilon_{in}$  : Turbulent Energy Dissipation Rate.  
 $\rho$  : Density ( $Kg/m^3$ ).  
 $\mu$  : Dynamic Viscosity ( $N.s/m^2$ ).  
 $\nu$  : Kinematic Viscosity ( $m^2/s$ ).  
 $\nu_t$  : Turbulent Viscosity.  
 $\theta$  : Angle of vertical deflection of grille (degree).  
 $\psi$  : Angle of horizontal deflection of grille (degree).

## Introduction

The simulation of room airflow has the potential to improve thermal comfort, indoor air quality, and the design of heating, ventilation, an air conditioning system. Information concerning the thermal condition of a room is helpful to the designer of heating or cooling systems, and can be provided by computational analysis of air velocity and temperature in a room<sup>[1]</sup>.

In Computational Fluid Dynamics (CFD), the designer has the capability to design and redesign a room over and over again at relatively low price compared with full scale experimentation<sup>[2]</sup>.

Awbi (1989) used the turbulence model to solve (2-D) and (3-D) ventilation problems to evaluate ceiling diffusers; velocity profiles and temperature distribution. Good agreement between experimental and numerical results is reached except for near the floor<sup>[3]</sup>. Haghghat et. al. (1989) discussed the use of the (k- $\epsilon$ ) turbulence model in simulating the convective flow in a partitioned conditioned space. The study also discusses the effect of door height and location on the pattern of airflow and temperature distribution. The results indicates that the flow pattern is quite

sensitive to the variations of the door height and location<sup>[4]</sup>.

Michael Ramey (1994) used a FORTRAN computer code, which simulates room airflow using laminar model and turbulent (k-ε) model with wall function and a turbulent low-Reynolds (k-ε). The room dimensions are (4.6×2.75×2.75)m. The prediction of convection coefficients and outlet temperatures were investigated and results are compared with experimental data<sup>[5]</sup>.

Florin Baltaretu (2001)<sup>[6]</sup> studied the numerical simulation of turbulent air flow in a ventilated room with ceiling slot air supply and return. Turbulent (k-ε) model with finite volume method and the SIMPLE computational algorithm are used to study the air flow in the room<sup>[7]</sup>. Tome Wilson, and Rana (2007)<sup>[7]</sup> have studied thermal comfort principles and physiological responses, theoretical and applied perspectives. Examine strategies to integrate advanced diagnostics with clear communication to explain how people and buildings interact and explore ways to achieve comfortable conditions.

**Numerical analysis**

All the equations used in this work has been deduced from Awbi<sup>[3]</sup>.

**Mass Conservation (continuity)**

$$\frac{\partial U_i}{\partial X_i} = 0 \dots\dots\dots(1)$$

***Momentum Equation***

$$\frac{\partial U_i}{\partial t} + \frac{\partial}{\partial x_j}(U_i U_j) = -\frac{1}{\rho} \frac{\partial P}{\partial x_i} + g_i + \nu \nabla^2 U_i \dots\dots\dots(2)$$

***Energy Equation***

$$\frac{\partial T}{\partial t} + \frac{\partial}{\partial x_j}(U_j T) = \alpha (\nabla^2 T) \dots\dots\dots(3)$$

**Solution Methodology**

This section details the solution methodology for the project including discussion on discretization, grid selection algorithm, and boundary conditions. This methodology was implemented through the FORTRAN computer program capable of modeling three-dimensional, turbulent, buoyant flow using finite-difference techniques.

**Turbulent model**

***Turbulent Flow Equation –Continuity***

$$\frac{\partial \bar{U}_i}{\partial x_i} = 0 \dots\dots\dots(4)$$

***Turbulent Flow Equation –Momentum***

$$\frac{\partial U_i}{\partial t} + \frac{\partial}{\partial X_j}(U_i U_j) = -\frac{\partial}{\partial X_i} \left( \frac{P}{\rho} \right) + g_i + \frac{\partial}{\partial X_j} \left( \nu_t \left( \frac{\partial U_i}{\partial X_j} + \frac{\partial U_j}{\partial X_i} - \frac{2}{3} K \delta_{ij} \right) \right) \dots\dots\dots(5)$$

The turbulent viscosity may be determined empirically from Eq. (6).

$$\nu_t = C_\mu \frac{k^2}{\epsilon} \dots\dots\dots(6)$$

where

: Constant (generally 0.09)  $C_\mu$

This program is based on General 3-dimension flow laminar, constant density code written by D.G Lilley<sup>[5]</sup> and modified by Michael Ramey<sup>[8]</sup> and A.A.M Saleh<sup>[9]</sup>.

**Solution Procedure**

Details of the approach used to solve for the velocities and scalar quantities are included in this section. First the geometry, grid spacing, initial conditions, some boundary specifications, physical properties, and other necessary information are read by the program. The program calculates additional geometric and numerical parameters such as the volume flow rate,

the number of air changes per hour (ACH), and the areas of the inlet and outlet. After initial values and boundary conditions are imposed, time advanced velocity components, temperature, turbulent energy and turbulent dissipation values are calculated for the entire 3-D domain. Boundary conditions are updated after the determination of time advanced values. Next, the continuity equation is satisfied using the change in pressure as a correction factor for the time advanced velocity components. After continuity is satisfied, residual terms for the velocities are calculated based on the amount of change in the values from the previous time step.

At this point in the solution process, a check for convergence is performed. If the values have not converged, then another time step must be performed. So, the time advanced values are shifted to the old memory locations, and time is advanced one step. Then, new time advanced values can be calculated. This process continues until convergence has been achieved.

### Marker-and-Cell Representation

The marker-and-cell (MAC), method was developed by Harlow and Welch<sup>[10]</sup> and it forms the basis for the finite difference techniques implemented in this study. The Marker-and-cell method defines all scalar quantities at the center of the appropriate cell face as shown in figure(1).

### Finite Difference Approximation

#### Turbulent Flow

As mentioned previously, the turbulent equation requires different finite difference representations than those approximating the laminar flow.

### Continuity Equation

Because the mean velocity values need only to be considered when imposing the continuity equation, the

finite - difference equation of Equation (7) may be used to impose the conservation of mass for turbulent as well as laminar flow.

$$\frac{1}{\Delta x} (U_{i,j,k} - U_{i-1,j,k}) + \frac{1}{\Delta y} (V_{i,j,k} - V_{i,j-1,k}) + \frac{1}{\Delta z} (W_{i,j,k} - W_{i,j,k-1}) = 0 \quad \dots\dots\dots(7)$$

### Momentum Equations

For convenience and ease of implementation into a numerical scheme, the momentum equations derived for turbulent flow Equation (5), will be re-written using a new term  $\Gamma_i$

$$\frac{\partial U_i}{\partial t} + \frac{\partial}{\partial X_j} (U_i U_j) = - \frac{\partial}{\partial X_i} \left( \frac{P}{\rho} \right) + g_i + \Gamma_i \quad \dots\dots\dots(8)$$

where

$$\Gamma_i = \frac{\partial}{\partial X_j} \left( \nu_t \left( \frac{\partial U_i}{\partial X_j} + \frac{\partial U_j}{\partial X_i} \right) - \frac{2}{3} k \delta_{ij} \right) \quad \dots\dots\dots(9)$$

### Turbulent Kinetic Energy Equation

The turbulent kinetic energy equation is given below.

$$\frac{\partial k}{\partial t} + \frac{\partial}{\partial X_j} (U_j k) = \Theta(k) + \nu_t \Pi - \varepsilon \quad \dots\dots\dots(10)$$

Where

$$\Pi = \frac{\partial U_i}{\partial x_j} \left[ \frac{\partial U_i}{\partial x_j} + \frac{\partial U_j}{\partial x_i} \right] \dots\dots(11)$$

$$\Theta(k) = \frac{\partial}{\partial X_j} \left[ \frac{\nu_t \partial k}{\sigma_k \partial X_j} \right] \quad \dots\dots\dots(12)$$

### Turbulent Dissipation Equation

Similar to the turbulent energy, the equation for the dissipation of turbulent energy may be written as:

$$\frac{\partial \varepsilon}{\partial t} + \frac{\partial}{\partial x_j} (U_j \varepsilon) = \Theta(\varepsilon) + \frac{C_1 F_1 v_t \varepsilon}{k} - C_2 F_2 \frac{\varepsilon^2}{k} + E$$

..... (13)

### Turbulent Solution Algorithm

The computer program developed for this project employ a method introduced by Hirt and Cook [11].

The mass divergence (D) at each cell can be calculated using the continuity equation as:

$$D = \frac{1}{\Delta x} (\tilde{U}_{i,j,k} - \tilde{U}_{i-1,j,k}) + \frac{1}{\Delta y} (\tilde{V}_{i,j,k} - \tilde{V}_{i,j-1,k}) + \frac{1}{\Delta z} (\tilde{W}_{i,j,k} - \tilde{W}_{i,j,k-1})$$

(14)

### Boundary Conditions

In this section, the potential focuses on the boundary condition allows at each of the three boundaries are described. The equation of these functions are given in table (1).

### Result and Discussion

The dimension of room selected in this study is (6×4×3)m as shown in figure (2). Many computational runs are performed at various air flow rates, blades angle of supply air grille. The summary of cases considered in this study is given in Table (2). Different computational runs are performed for all cases after 120 second, two-dimensional velocity vector plots and temperature contour lines are presented in this study.

Figure (3) show the velocity pattern for (5 ACH) and the stagnant zone under inlet is also clear in same figure. The differences between the low and high velocity air flow patterns are lighted with the plots of (15 ACH). Figure (4)

show more air movement along the far wall for (15 ACH). Figures (5) to (6) show the contour line of temperature distribution for the (5, 15 ACH). It is clear that the core of the air jet has the minimum temperature approach the inlet temperature. Figures (7) and (8) show the velocity and temperature distribution of a side wall grille with a (15°) upward deflection located slightly below a ceiling. The jet adjacent ceiling provides some "Coanda" effect, increasing the throw beyond it. The stagnant zone is located under supply grille and in the far upper corner opposite wall. Figures (9) and (10) show the velocity distribution and temperature contour lines of a side wall grille with angle (15°) downward. Figure (11) shows air distribution performance index (ADPI). High significant difference in ADPI with change in blade angle of grille, and the best of (ADPI) occurs when the blades angle of grille deflected (15°) down because the air jet enters the room and attaches itself to the floor and eventually a full re-circulation pattern occurs. Increasing the (ACH) decreases the (ADPI) because increasing in ACH means increasing in velocity which may be out of limits of comfort conditions in the room (high draft zone).

### Conclusions

- 1- Using side wall grilles inlet with variable angles in room best air velocity and temperature distributions (ADPI) occur when (ACH) is about (10), and deflection angle of grille is (15 down).
- 2- Even when high (ACH) produces good air mixing and uniform temperature stratification, it can lead to discomfort, the same action occurs when the low (ACH) applied produces bad air mixing and discomfort.

- 3- The jet adjacent ceiling provides some "Coanda" effect, increasing the throw beyond it.

### References

1. Jalal M. Jalil, Journal of Engineering, "Three Dimensional Transient, Turbulent, Buoyant Air Distribution inside room", University of Al- Mustansiria, Volume 6-NO.5, 2002.
2. Hanaa Muhsen Mohammed Ali "Numerical Study of Isothermal and Non- Isothermal flow in Ventilated Rooms" M.Sc Thesis, University of Technology\Baghdad, 2003.
3. H. B. Awbi, "Application of computational fluid dynamics in room ventilation", Building and Environment, Vol.24, pp.73-84, 1989.
4. Haghghat, F, Z. Jiang and J. C. Y Wang, "Natural Convection and Air Flow Pattern in a Partitioned Room with Turbulent Flow", ASHRAE Journal, pp. 600-610,1989.
5. Michael Ramey, J. Spitler, "Application of Computational Fluid Dynamics to Indoor Room AirFlow", M.sc. Theses, Okiahoma Christian University, 1994.
6. Florin Baltaretu, "Numerical prediction of air flow pattern in a ventilated room", Analele University, PP.11-16, 2001
7. Tom Wilson, and Rana Belshe, "COMF1 Principle of thermal comfort", Cleveland, Ohio, 2007.
8. Lilley, D. G., "Three Dimensional Flow Prediction for Industrial Mixing", ASME International Computers In Engineering Conference, San Francisco, CA, 1988.
9. Ahmed A. M. Saleh, "Experimental and Numerical Study on the Effect of Velocity and Temperature Distributions in a Large Space", PhD Thesis, University of Technology \ Baghdad, 2005.
10. F. H. Harlow, and J. E. Welch, (1965), Numerical Calculation of Time Dependent Viscose Incompressible flow

of Fluid with Free Surface, the physical of fluid, vol.8, No.13, pp. (2182-2189).

11. Hirt, C. W. and J. L. Cook, (1972), Calculation Three Dimensional Flows Around Structures and Over Rough Terrain, Journal of Computational Physics, Vol. 10, PP. 324-340.

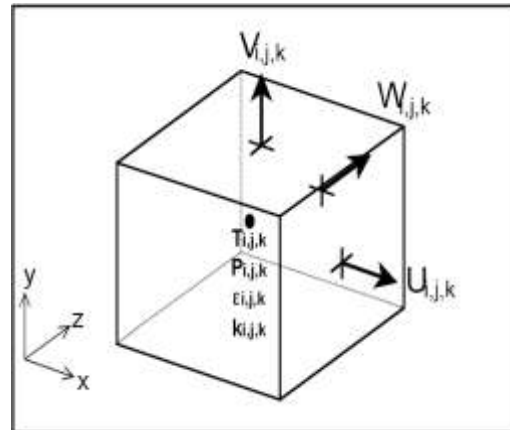


Figure (1) Marker -and- Cell Representation

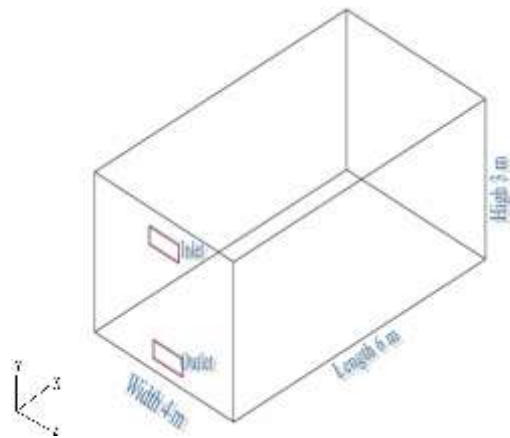


Figure (2) Room scale Layout (Normal)

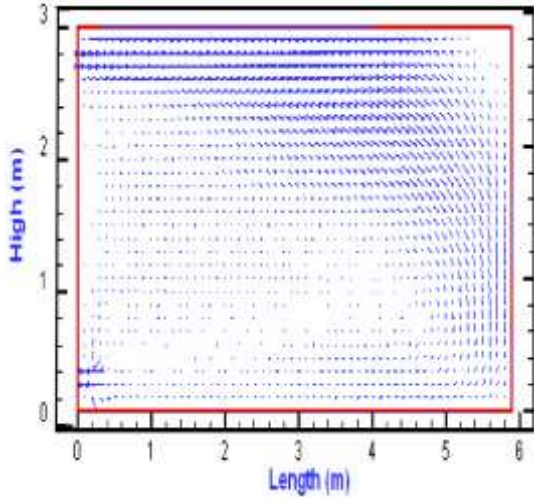


Figure (3) Velocity Distribution at 5 ACH, Angle (0 deg.) & (16 °C) Tin

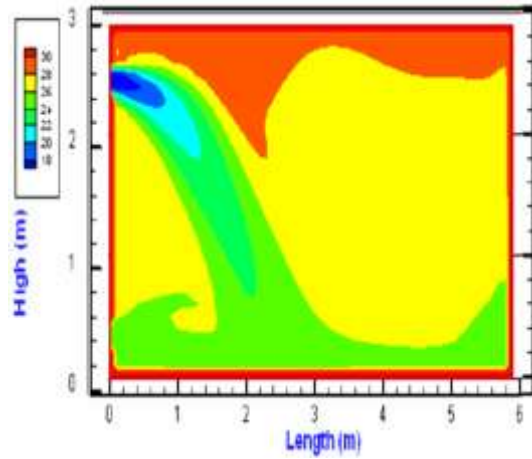


Figure (6) Temperature contours at 15 ACH, Angle (0 deg.) & (16 °C) Tin

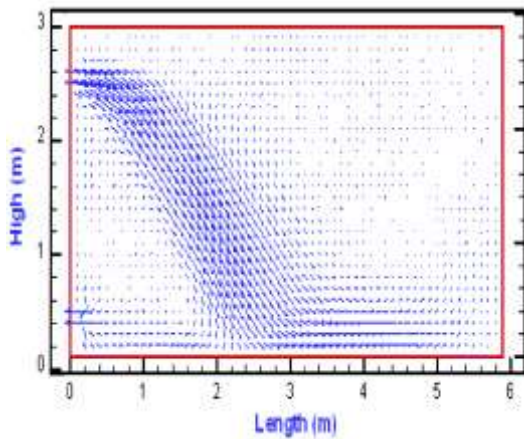


Figure (4) Velocity Distribution at (15ACH), Angle (0 deg.) & (16 °C) Tin

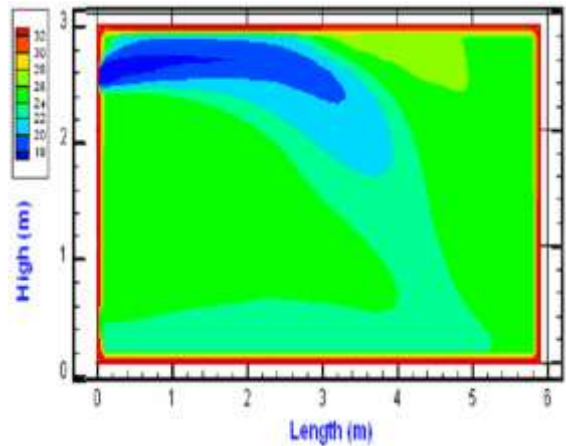


Figure (7) Velocity Distribution at (10 ACH), Angle (15° up) & (16 °C)

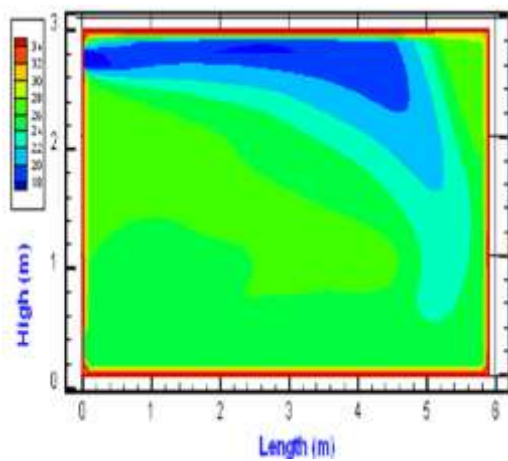


Figure (5) Temperature contours at (5 ACH), Angle (0 deg.) & (16 °C) Tin

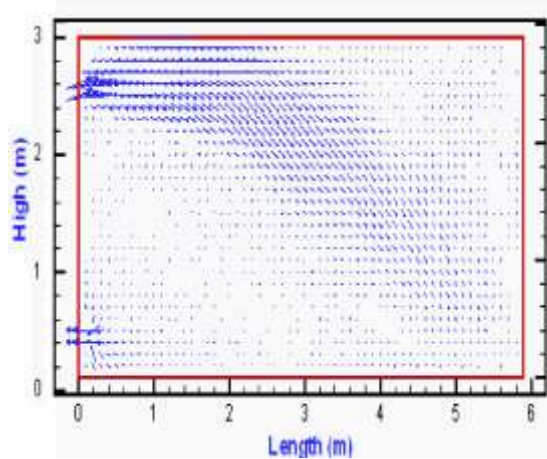


Figure (8) Temperature contours at (10 ACH), Angle (15° up) & (16 °C)



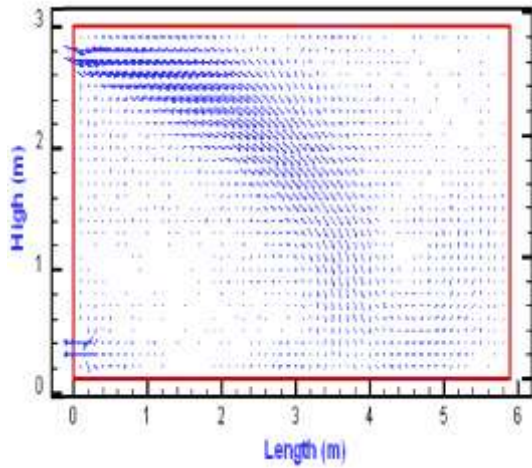
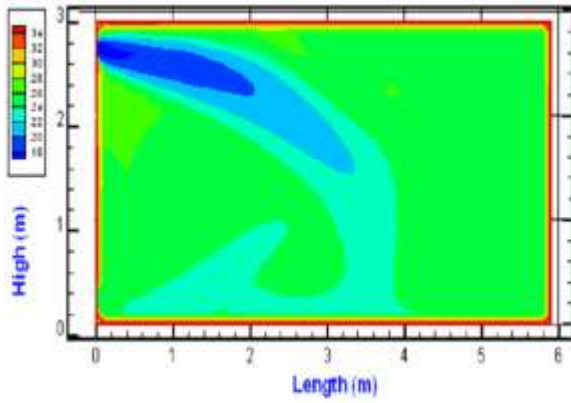


Figure (9) Velocity distribution at (10 ACH), Angle (15° down) & (16° C) Tin



Figure(10)Temperature contours at (10 ACH) Angle (15° down) &(16°C) Tin

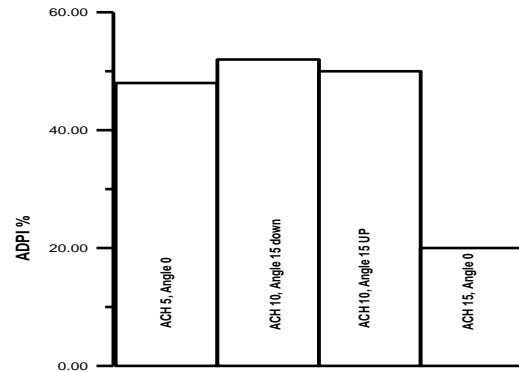


Fig. (11) Air Distribution Performance Index (ADPI)



**Table (1) Boundary Conditions**

| Boundary              | Velocities   | Temperature                           | Turbulent Energy                       | Turbulent Dissipation                            |
|-----------------------|--|---------------------------------------|--|--|
| <b>Inlet</b>          | $U_t = 0$ $U_n = U_{jet}$ $U = U_{in} \times \cos(\theta)$ $V = U_{in} \times \sin(\theta)$ $W = U_{in} \times \sin(\psi)$ | $T_{in}$                              | $k_{in} = \frac{3}{2} I_u^2 U_{jet}^2$ | $\epsilon_{in} = \frac{k_{in}^{3/2}}{\lambda H}$ |
| <b>Outlet</b>         | $U_t = 0$ $U_n = U_{jet} \frac{A_{in}}{A_{out}}$   | $\frac{\partial T}{\partial x_n} = 0$ | $\frac{\partial k}{\partial x_n} = 0$  | $\frac{\partial \epsilon}{\partial x_n} = 0$     |
| <b>Wall No slip</b>   | $U_t = 0 \quad U_n = 0$  | $T_1 = 2 \times T_{wall} - T_2$       |  |  |
| <b>Wall Free slip</b> | $\frac{\partial U_t}{\partial x_n} = 0 \quad U_n = 0$  |                                       |  |  |
| <b>Wall Function</b>  | $U_n = 0$ $\frac{\partial U_t}{\partial x_n} \Big _w = \frac{m U_t}{y_n}$  |                                       |  |  |

**Table (2) Summary of Numerical Cases Studied**

| ACH | Inlet Temp. (°C) | Case specification | Angles   |
|-----|------------------|--------------------|----------|
| 5   | 16               | Normal             | 0        |
| 15  | 16               | Normal             | 0        |
| 10  | 16               | With angle         | UP 15°   |
| 10  | 16               | With angle         | Down 15° |